Accepted Manuscript

Glucosylation of flavonoids and flavonoid glycosides by mutant dextransucrase from *Lactobacillus reuteri* TMW 1.106

Tizian Klingel, Martina Hadamjetz, Anja Fischer, Daniel Wefers

PII: S0008-6215(19)30278-2

DOI: https://doi.org/10.1016/j.carres.2019.107741

Article Number: 107741

Reference: CAR 107741

To appear in: *Carbohydrate Research*

Received Date: 2 May 2019

Revised Date: 9 July 2019

Accepted Date: 9 July 2019

Please cite this article as: T. Klingel, M. Hadamjetz, A. Fischer, D. Wefers, Glucosylation of flavonoids and flavonoid glycosides by mutant dextransucrase from *Lactobacillus reuteri* TMW 1.106, *Carbohydrate Research* (2019), doi: https://doi.org/10.1016/j.carres.2019.107741.

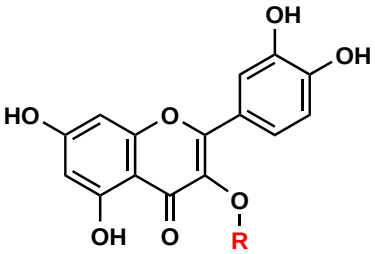

Sucrose

L. reuteri TMW 1.106
L242A dextransucrase

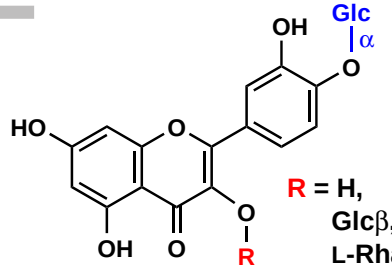

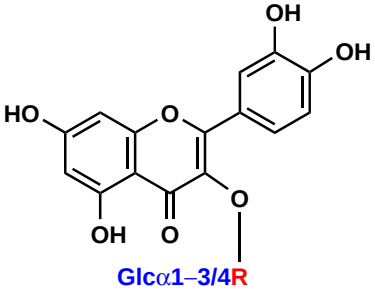

R = Glcβ

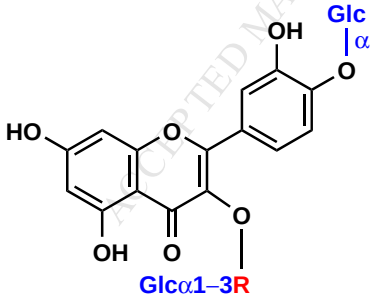

R = Glcβ

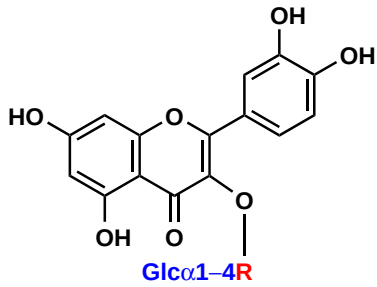

R = L-Rhaα1–6Glcβ

Glucosylation of flavonoids and flavonoid glycosides by mutant dextransucrase from *Lactobacillus reuteri* TMW 1.106

Tizian Klingel[1], Martina Hadamjetz[1], Anja Fischer[1], Daniel Wefers[1]*

[1] Department of Food Chemistry and Phytochemistry, Institute of Applied Biosciences, Karlsruhe Institute of Technology (KIT), Adenauerring 20a, 76131 Karlsruhe, Germany

*Correspondence: Daniel Wefers, Department of Food Chemistry and Phytochemistry, Institute of Applied Biosciences, Karlsruhe Institute of Technology (KIT), Adenauerring 20a, 76131 Karlsruhe, Germany. daniel.wefers@kit.edu, Phone: +49 721 608 42929, Fax: +49 721 608 47255

ABSTRACT

Flavonoids are commonly abundant, plant-derived polyphenolic compounds which are responsible for color, taste, and antioxidant properties of certain plant based food. Glucosylation by glucansucrases or other glycosyltransferases/glycoside hydrolases has been described to be a promising approach to modify stability, solubility, bioavailability, and taste profile of flavonoids and related compounds. In this study, we modified and applied a recombinant dextransucrase from *Lactobacillus reuteri* TMW 1.106 to glucosylate various flavonoids and flavonoid glycosides. The glucoconjugates were subsequently isolated and characterized by using two-dimensional NMR spectroscopy. Efficient glucosylation was achieved for quercetin and its glycosides quercetin-3-*O*-β-glucoside and rutin. Significant portions of α-glucose conjugates were also obtained for epigallocatechin gallate, dihydromyricetin, and cyanidine-3-*O*-β-glucoside, whereas glucosylation efficiency was low for naringin and neohesperidin dihydrochalcone. Most of the flavonoids with a catechol or pyrogallol function at the B-ring were predominantly glucosylated at position *O*4'. However, glycosyl substituents such as β-glucose, rutinose, or neohesperidose were glucosylated at varying positions. Therefore, mutant dextransucrase from *L. reuteri* TMW 1.106 can be applied for versatile structural modification of flavonoids.

KEYWORDS

glucansucrase, modification, NMR spectroscopy, acceptor reaction, structural characterization, purification.

ABBREVIATIONS

L. = *Lactobacillus*, HSQC = Heteronuclear Single Quantum Coherence, COSY = H,H-Correlated Spectroscopy, H2BC = Heteronuclear Two-bond Correlation, TOCSY = Total Correlated Spectroscopy, HMBC = Heteronuclear Multiple Bond Correlation.

1 INTRODUCTION

Flavonoids are a very heterogeneous group of polyphenolic secondary plant metabolites which are widely distributed among different plants. Consumption of polyphenol-rich foods was associated with beneficial health effects which were discussed to be related to the antioxidant activity of flavonoids [1]. In addition, some flavonoids also affect the sensory properties of plant based food. For example, anthocyanins are responsible for the color of many fruits, whereas some flavonoids such as the flavanone naringin contribute to the bitter taste of some citrus fruits [2]. Furthermore, the flavonoid derivative neohesperidin dihydrochalcone is added to food products as a sweetener or flavor enhancer [3]. In nature, flavonoids are often glycosylated at varying positions such as position *O*3 (if present) or position *O*7 and *O*5 [4]. It has already been demonstrated that glycosylation significantly influences the solubility, stability, bioavailability, and antioxidant properties [4-7]. Therefore, enzymatic *in vitro* glycosylation has also been investigated as an approach to modify the described properties. Besides cyclodextrin glucanotransferases, α-glucosidases, and maltogenic amylases [5, 7-13], glucansucrases have already been applied to glucosylate selected flavonoids [14-20]. These enzymes belong to the GH70 family and normally catalyze the conversion/incorporation of sucrose into polymeric α-glucans, but by selecting appropriate reaction conditions, oligosaccharides or other hydroxyl group containing compounds can also be conjugated with α-glucose [21]. However, the above mentioned studies focused on glucosylation of non-glycosylated flavonoids such as luteolin, quercetin, myricetin, dihydromyricetin, and epigallocatechin gallate. In addition, only glucansucrases from *Leuconostoc mesenteroides* have been used for flavonoid glucosylation. However, recombinant glucansucrases from *L. reuteri* have been successfully applied for glucosylation of steviol glycosides or simple phenols such as catechol [22-26]. Furthermore, site directed mutagenesis was applied to improve glucosylation of these substrates and other non-carbohydrate molecules [23, 24, 26].

In previous studies, it was demonstrated that dextransucrase from *Lactobacillus (L.) reuteri* TMW 1.106 synthesizes *O*4-branched dextrans and thus produces a rather rare dextran type [27, 28]. Furthermore, we observed a high expression level and thus a comparably high enzyme activity after cloning of the encoding gene into a pET-based expression vector and heterologous expression of the recombinant sucrase in *E. coli*. Consequently, this recombinant dextransucrase is a promising candidate for the modification of polyphenolic compounds. Therefore, the aim of this study was to analyze the structures of α-glucose conjugates formed by the incubation of different flavonoids, flavonoid glycosides, and flavonoid derivatives with dextransucrase from *L. reuteri* TMW 1.106.

2 RESULTS AND DISCUSSION

Several flavonoid substrates which showed a high structural heterogeneity of both the flavonoid residues as well as the attached sugars were used for the glucosylation experiments (Fig. S1). Besides the unglucosylated flavonole quercetin, quercetin-3-*O*-β-glucoside and rutin (which corresponds to quercetin-3-*O*-rutinoside) were also used as substrates. Furthermore, the plant pigment cyanidin-3-*O*-β-glucoside was isolated from blackberry and used for the glucosylation experiments. With regards to taste-active flavonoids/flavonoid derivatives, naringin and neohesperidin dihydrochalcone were used as substrates. These compounds carry a neohesperidose residue at position *O*7, thus they show a different type and location of the sugar side chain than the previously mentioned substrates. In addition, dihydromyricetin (ampelopsin) and epigallocatechin gallate were used. In contrast to all other substrates, these non-glycosylated flavonoids both carry a pyrogallol group at the B-ring (and, in case of epigallocatechin gallate, at position *O*3 in form of gallic acid). Therefore, the substrates used in this study exhibit different flavonoid types, different substitution patterns of the flavonoid B-ring, and differences in the type and position of the flavonoid-bound sugar units.

In preliminary experiments, wildtype dextransucrase from *L. reuteri* TMW 1.106 was successfully applied for glucosylation of some flavonoid substrates, but a rather low glucosylation efficiency was achieved. Devlamynck, te Poele, Meng, van Leeuwen and Dijkhuizen [26] demonstrated that modification of certain amino acids in the +1 and +2 acceptor binding site of glucansucrase Gtf180 from *L. reuteri* 180 eventually led to an increased glucosylation of non-carbohydrate molecules by suppressing synthesis of polymeric α-glucans. Therefore, we aligned the amino acid sequence of *L. reuteri* TMW 1.106 dextransucrase and Gtf180 to identify the leucine residue equivalent to L981 in Gtf180 (Fig. S2). Subsequently, we changed this leucine residue to alanine by using site-directed mutagenesis (yielding *L. reuteri* TMW 1.106 L242A). The mutant *L. reuteri* TMW 1.106 dextransucrase showed a clearly increased glucosylation activity and was thus used for all further experiments. To evaluate incubation conditions which allow for the isolation of conjugate amounts suitable for structure elucidation by NMR spectroscopy, different amounts of substrate, sucrose, and enzyme were tested in a small-scale. It was concluded that the highest amount of conjugates can be obtained by using the highest acceptor concentration possible (with regards to solubility), 500 mM sucrose, and 100 mU mutant *L. reuteri* TMW 1.106 dextransucrase / mL substrate solution. Therefore, these conditions were used for the glucosylation of all substrates.

To obtain information on the portion and the molecular masses of the conjugates formed, the incubation mixtures were analyzed by HPLC-DAD/MS. As a first approximation, conjugation efficiency can be derived from the UV/Vis absorption signal intensity. However, changes in the UV/Vis response due to conjugation need to be considered. The conjugates were named after the substrate (prefix) and the number of added α-glucosyl moieties (suffix, derived from the *m/z* of the individual conjugates). For unambiguous structural elucidation, conjugates were isolated by preparative HPLC and characterized by using several one- and two-dimensional NMR experiments. Although the proton spectra yield valuable information on the flavonoid

derived protons, sugar-derived protons can often not be resolved due to signal overlap. However, a Heteronuclear Single Quantum Coherence (HSQC) experiment mostly allows for the resolution of all signals, because they are spread into the ^{13}C dimension. To identify downfield shifted HSQC signals due to α-glucose substitution, spectra of the untreated compounds were also recorded. Identification and assignment of the individual HSQC signals was achieved by using H,H-Correlated Spectroscopy (COSY), Heteronuclear Two-bond Correlation (H2BC), Total Correlated Spectroscopy (TOCSY), and HSQC-TOCSY experiments. Eventually, unambiguous information on interglycosidic linkages and on substitution of the flavonoid residues was obtained from the Heteronuclear Multiple Bond Correlation (HMBC) spectra. The ^{1}H and ^{13}C chemical shifts of all flavonoids and their conjugates are provided in the supplementary data (Tab. S1-S8).

3.1 Quercetin and quercetin glycosides

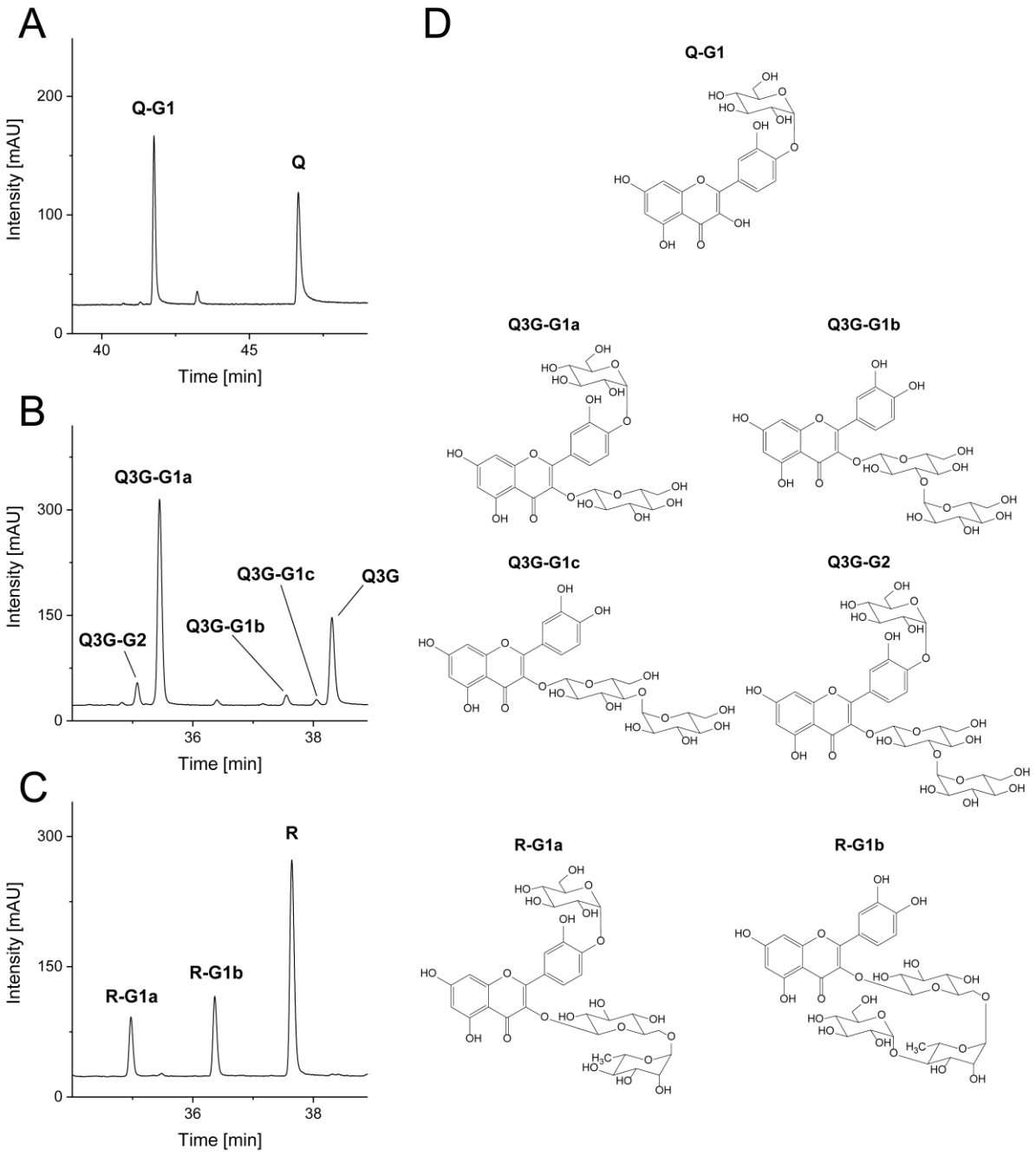

Fig. 1: HPLC-DAD/MS chromatograms of incubations of quercetin (Q, final concentration: 3 mM, subfigure A), quercetin-3-*O*-β-glucoside (Q3G, final concentration: 5 mM, subfigure B), and rutin (R, final concentration: 3 mM, subfigure C) with 100 mU / mL mutant *L. reuteri* TMW 1.106 dextransucrase and 500 mM sucrose. The structures of the conjugates (subfigure D) were determined by NMR spectroscopy.

119

120 One major monoglucosylated conjugate (Q-G1) was obtained after incubation of quercetin with
121 mutant *L. reuteri* TMW 1.106 dextransucrase (Fig. 1A). According to the peak areas, this
122 conjugate was present in about equal amounts than quercetin which indicates a high conjugation
123 efficiency (assuming an at least roughly comparable UV response). In accordance with its
124 molecular mass, signals of one α-glucose were detected in the HSQC spectrum of the isolated
125 compound. This sugar unit was identified by its characteristic ^{1}H and ^{13}C chemical shifts and
126 the $^{3}J_{HH}$ coupling constant of the anomeric proton. With regards to the quercetin unit, a
127 downfield shift of C5'H5' and C6'H6' was observed compared to unmodified quercetin.
128 Furthermore, H1 of glucose as well as H2', H5', and H6' of quercetin showed an HMBC
129 correlation at 146.5 ppm. Because of this ^{13}C chemical shift and because of the absence of
130 another HMBC signal between 145 and 150 ppm, these results show that the B-ring is
131 substituted at position *O*4' (Fig. 1D). This conclusion was based on previous NMR data on
132 quercetin α-glucosides [17]. As reported by Moon, Lee, Jhon, Jun, Kang, Sim, Choi, Moon and
133 Kim [17], substitution at position *O*4' leads to almost identical ^{13}C chemical shifts of C3' and
134 C4' (146.4 and 146.9 ppm), whereas substitution at position *O*3' results in two distinct ^{13}C
135 chemical shifts for C3' (144.8 ppm) and C4' (149.8 ppm). This is also in good agreement with
136 NMR data from our laboratory for glucosylated phenolic acids with a catechol function.
137 Notably, the HPLC chromatogram also contained very low portions of another
138 monoglucosylated product (retention time 43 min) which most likely corresponds to the *O*3'
139 substituted conjugate. However, from the very low abundance of this conjugate, it can
140 concluded that position *O*4' of quercetin is highly preferred. In previous reports, glucansucrases
141 from *Leuconostoc mesenteroides* B-1299CB and *Leuconostoc mesenteroides* NRRL B-512F
142 were also reported to prefer position *O*4' over position *O*3', but compared to our results, higher
143 portions of *O*3' glucosylated quercetin were detected [14, 17]. Furthermore, Malbert, Moulis,

Brison, Morel, Andre and Remaud-Simeon [20] obtained several mono- and oligoglucosylated products by using a branching sucrase from *Leuconostoc mesenteroides* B-1299. However, the selective glucosylation of quercetin at position *O*4' observed for mutant *L. reuteri* TMW 1.106 dextransucrase may be advantageous for some applications. The glucosylation efficiencies described for the previously used wildtype glucansucrases showed broad variation from 4 % [14] to 25 % [17] and 50 % [20]. In addition, some mutants of the branching sucrase yielded glucosylation efficiencies of even about 90 % [20]. Therefore, mutant *L. reuteri* TMW 1.106 dextransucrase provides a high glucosylation efficiency (about 50 % based on the peak areas) compared to some other enzymes, but a higher efficiency may be achieved by creating and screening more mutants.

Conjugation of quercetin-3-*O*-β-glucoside also resulted in one major product (Q3G-G1a in Fig 1B) which was isolated from the reaction mixture. In addition, it was possible to purify one diglucosylated product (Q3G-G2) and two other monoglucosylated conjugates (Q3G-G1b and Q3G-G1c).

Just as for Q-G1, comparison of the main product Q3G-G1a with unmodified quercetin-3-*O*-β-glucoside showed that the HSQC signals derived from the B-ring of quercetin showed significantly different chemical shifts. Furthermore, the chemical shifts of the additional α-glucose unit were in good agreement with the chemical shifts of the α-glucose unit in Q-G1, suggesting a similar chemical environment. Eventually, the attachment of α-glucose to position *O*4' of the B-ring was confirmed by an HMBC correlation between H1 of glucose and C4' of quercetin at 5.41 / 147.0 ppm.

For the two monoglucosylated conjugates Q3G-G1b and Q3G-G1c, quercetin derived HSQC signals were not significantly altered, suggesting substitution of the β-glucose unit. After assignment of the HSQC signals by using COSY/TOCSY spectra, characteristic chemical shifts of the β-glucose derived signals were used to assign the substitution position of the β-glucose

unit (Fig. S3). Q3G-G1b showed a significantly downfield shifted C3H3 signal (3.44 / 84.8 ppm), whereas Q3G-G1c showed a downfield shifted C4H4 signal (3.38 / 79.1 ppm). Therefore, these two monoglucosylated conjugates result from substitution of β-glucose at position *O*3 and *O*4, respectively.

As expected, the diglucosylated conjugate Q3G-G2 showed two sets of α-glucose derived signals (Fig. 2). From the characteristically shifted HSQC signals of quercetin and the chemical shifts of one α-glucose unit, it was concluded that quercetin is substituted at position *O*4' of the B-ring. The attachment of the corresponding glucose unit to position *O*4' of quercetin was also confirmed by an HMBC correlation between H1 of glucose and C4' of quercetin. The chemical shifts of the β-glucose unit and the remaining α-glucose unit were in good agreement with the chemical shifts observed for α/β-glucose in Q3G-G1b. Only the C1H1 and C2H2 signals of β-glucose were slightly shifted which is most likely a result of the B-ring substitution. However, the attachment of the second α-glucose to position *O*3 of β-glucose was clearly demonstrated by the diagnostic C3H3 signal of β-glucose (Fig. 2) and an HMBC correlation between H1 of α-glucose and C3 of β-glucose.

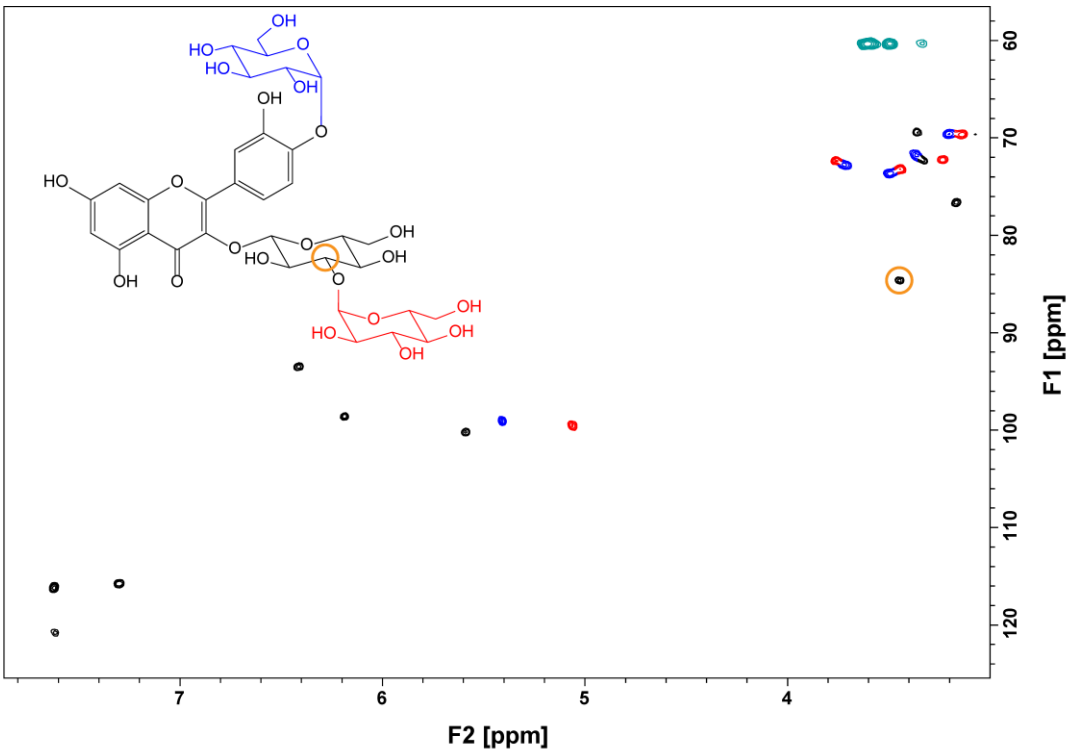

Fig. 2: HSQC spectrum and structure of the diglucosylated conjugate of quercetin-3-*O*-β-glucoside (Q3G-G2). Signals belonging to the two α-glucose residues are colored in red and blue. The diagnostic, downfield shifted C3H3 signal of the β-glucose unit is encircled in orange.

The predominant abundance of Q3G-G1a which is glucosylated at position *O*4' of the B-ring demonstrates that the preference for this position is not altered by the β-glucosyl residue at position *O*3 of quercetin. Furthermore, the other three monoglucosylated conjugates show that glucosylation can appear at different positions of the β-glucosyl residue. In addition, already glucosylated compounds can be further substituted with α-glucose which results in the formation of Q3G-G2. From the peak intensities in the chromatogram, a comparably high glucosylation efficiency can be derived, because more than half of quercetin-3-*O*-β-glucoside is glucosylated.

When rutin was incubated with mutant *L. reuteri* TMW 1.106 dextransucrase, only two monoglucosylated conjugates were detected. For R-G1a, the rutinose derived HSQC signals were in good agreement with unsubstituted rutin. Furthermore, ^{1}H and ^{13}C chemical shifts of quercetin as well as the additional α-glucose unit were in good agreement with the chemical shifts obtained for Q3G-G1a. Therefore, R-G1a is glucosylated at position *O*4' which was also confirmed by an HMBC correlation between H1 of glucose and C4' of quercetin.

For R-G1b, the quercetin signals were unmodified compared to the standard. In addition, assignment of the rutinose HSQC signals demonstrated that the chemical shifts of β-glucose were not significantly altered. However, α-rhamnose showed a clearly downfield shifted signal at 3.22 / 81.8 ppm. This signal was identified as C4H4 by using the COSY spectrum as well as an HMBC correlation between C4 and the characteristically located H6 of α-rhamnose (Fig. 3). From an HMBC correlation between C4 of the α-rhamnose unit and H1 of the α-glucose unit, it was also unambiguously demonstrated that the α-glucose unit is attached to this position.

These results demonstrate that the addition of a disaccharide to position *O*3 of quercetin does not impede glucosylation at position *O*4', but prevents glucosylation of the β-glucose unit. Furthermore, the glucosylation efficiency seems to be lowered, as the major part of rutin remained unmodified under the conditions used. However, glucosylation of the rhamnosyl residue at position *O*4 is an interesting novel feature of glucansucrases.

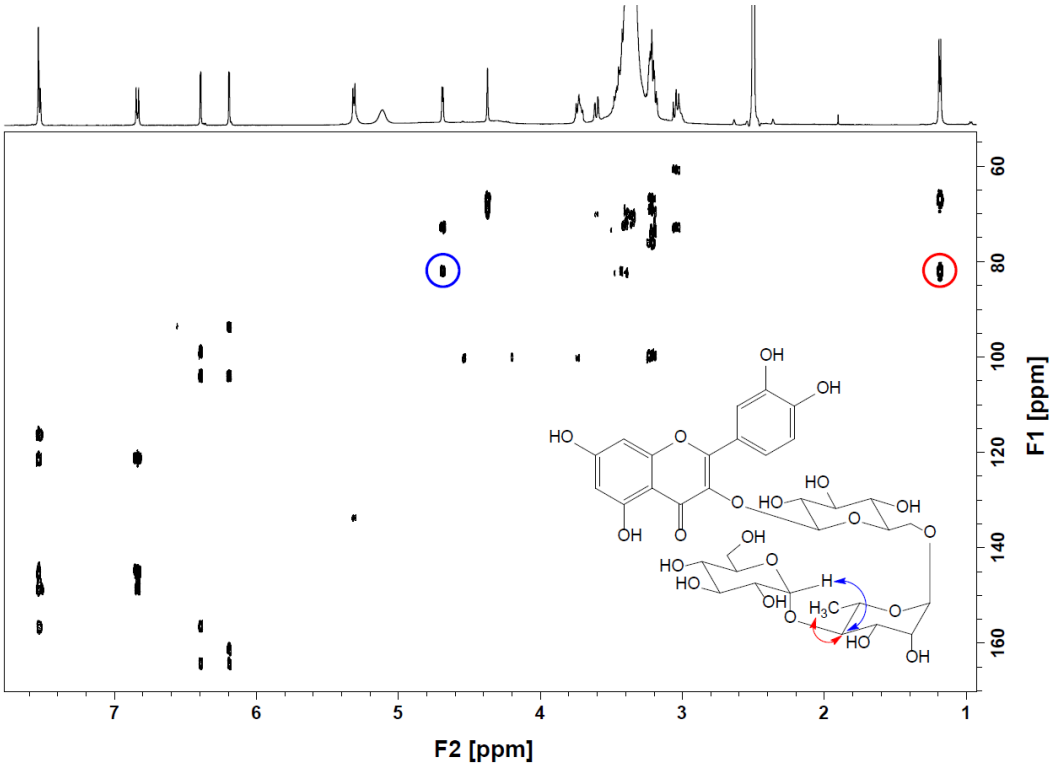

Fig. 3: HMBC spectrum and structure of the monoglucosylated conjugate of rutin (R-G1b). Diagnostic signals which helped to identify C4 of α-rhamnose and demonstrate the attachment of α-glucose to position *O*4 of α-rhamnose are encircled in red and blue.

3.2 Cyanidin-3-glucoside

The chromatogram obtained for the cyanidin-3-*O*-β-glucoside incubation mixture contained one additional, earlier eluting peak (Fig. 4).

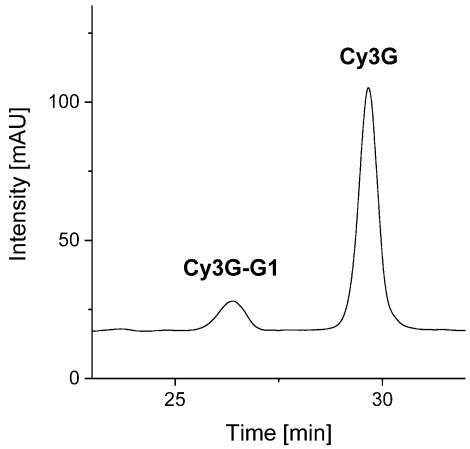

Fig. 4: HPLC-DAD/MS chromatogram of the incubation of cyanidin-3-*O*-β-glucoside (Cy3G, final concentration: 8 mM) with 100 mU / mL mutant *L. reuteri* TMW 1.106 dextransucrase and 500 mM sucrose. The structure of the monoglucosylated conjugate Cy3G-G1 is shown in Fig. 5.

The compound (Cy3G-G1) showed a quasimolecular ion at *m/z* 611 which demonstrates monoglucosylation of cyanidin-3-*O*-β-glucoside. For structural elucidation, the conjugate was isolated by preparative HPLC and NMR spectra were recorded in methanol-*d*4 with 0.1 % DCl. This solvent was used because it provides complete solubilization and well resolved spectra of the flavylium cation form. As expected, the HSQC spectrum contained signals typical for an α-glucose in addition to the signals of cyanidin-3-*O*-β-glucoside. Besides the slightly shifted C4H4 signal, the HSQC signals of cyanidin showed identical chemical shifts than for

unmodified cyanidin-3-*O*-β-glucoside. Thus it can be concluded that the β-glucose residue is glucosylated. After assigning the HSQC signals of the β-glucose unit by using COSY/TOCSY experiments, it was observed that the C6H6 signals showed a characteristic downfield shift (Fig 5).

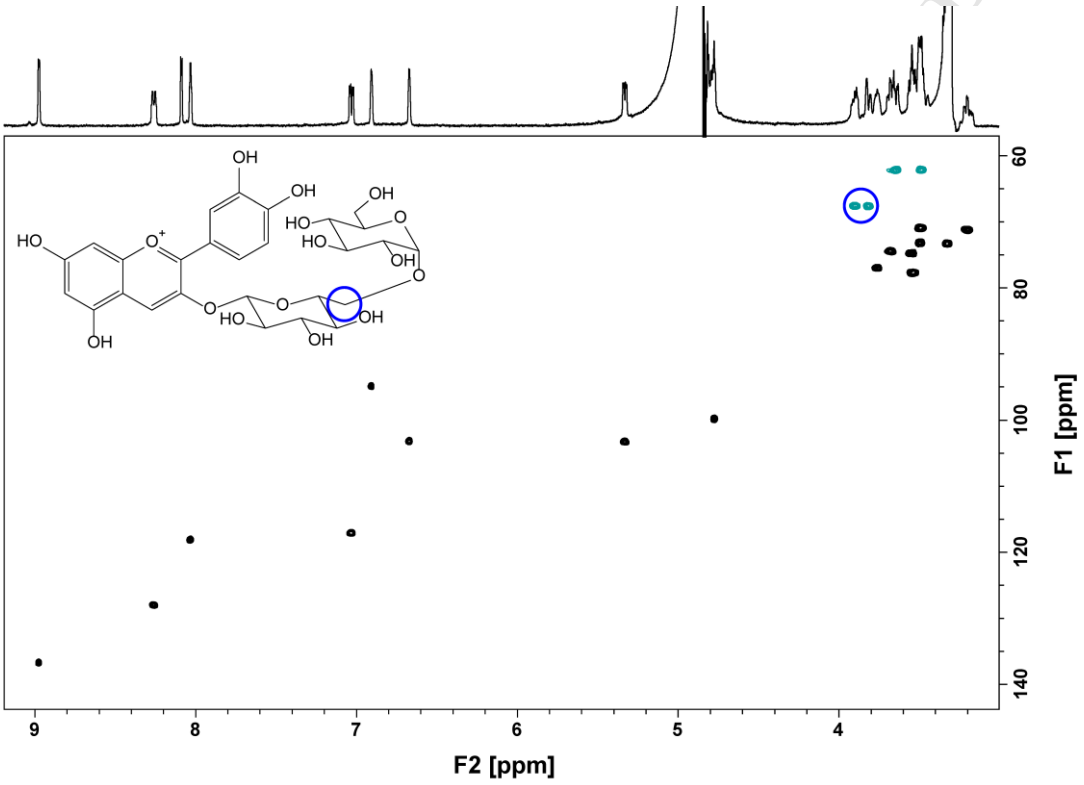

Fig. 5: HSQC spectrum and structure of the monoglucosylated conjugate of cyanidin-3-*O*-β-glucoside (Cy3G-G1). The diagnostic, downfield shifted C6H6 signals of the β-glucose unit are encircled in blue.

These downfield shifted signals strongly suggest substitution at position *O*6 of the β-glucose unit, which was eventually confirmed by an HMBC correlation between C6 of the β-glucose and H1 of the α-glucose. Therefore, cyanidin-3-*O*-β-glucoside shows a significantly different product spectrum than the structurally related quercetin-3-*O*-β-glucoside which was

253 glucosylated at position *O*4' of the B-ring and at positions *O*3 and *O*4 of β-glucose. Most likely,
254 the structural differences between the two compounds result in a different orientation of
255 cyanidin-3-*O*-β-glucoside in the active site of the enzyme.

256

257 **3.3 Naringin and neohesperidin dihydrochalcone**

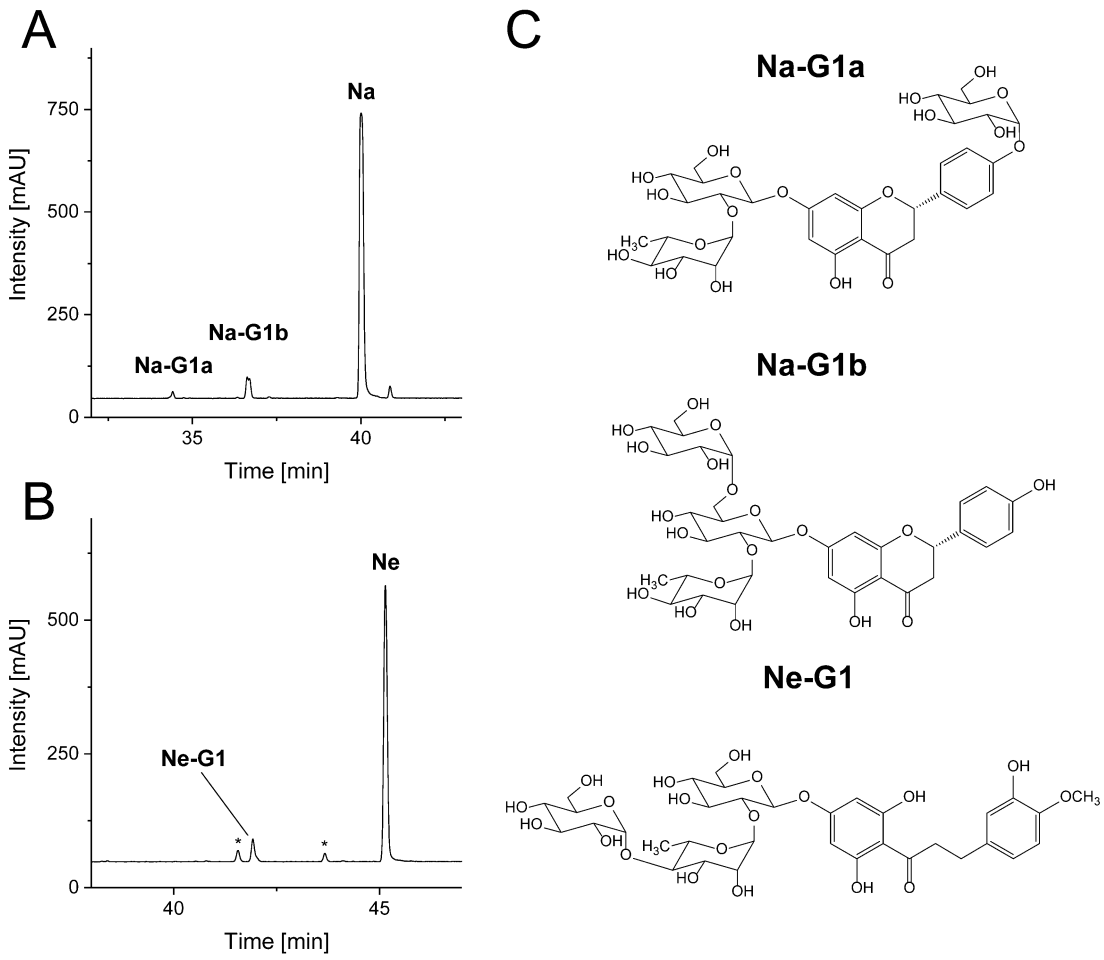

258

259 **Fig. 6:** HPLC-DAD/MS chromatograms of incubations of naringin (Na, final concentration: 30
260 mM, subfigure A) and neohesperidin dihydrochalcone (Ne, final concentration: 50 mM,
261 subfigure B) with 100 mU / mL mutant *L. reuteri* TMW 1.106 dextransucrase and 500 mM
262 sucrose. The peaks marked with an asterisk in subfigure B were also present in the untreated
263 neohesperidin dihydrochalcone preparation (see text). The structures of the conjugates
264 (subfigure C) were determined by NMR spectroscopy.

Two monoglucosylated conjugates were detected in the incubation mixture of naringin with mutant *L. reuteri* TMW 1.106 dextransucrase (Fig. 6A). However, the peak intensity suggested that the conjugates are lowly abundant and that glucosylation efficiency is rather low. Nevertheless, it was possible to isolate and characterize the two conjugates. The HSQC spectrum of Na-G1a yielded unmodified neohesperidose signals and the anomeric signal of the α-glucose showed a comparably high ^{1}H chemical shift. This was already observed for quercetin (glycoside) conjugates which are glucosylated at position *O*4' of the B-ring. Because the C2'H2', C3'H3', C5'H5', C6'H6' of naringin were also shifted downfield, it can be concluded that naringin is glucosylated at the hydroxyl group of the B-ring. The attachment of α-glucose to the B-ring was also confirmed by an HMBC correlation between H1 of α-glucose and C4' of naringin (Fig. S4).

The second monoglucosylated conjugate Na-G1b did not show any signal drift for the HSQC signals derived from the aglycone and the α-rhamnose unit. However, just as for the conjugate of cyanidin-3-*O*-β-glucoside, C6H6 signals of the naringin-bound β-glucose unit showed a characteristic ^{13}C downfield shift to 66 ppm (Fig. S5). Therefore it can be concluded that the additional α-glucose unit is bound to position *O*6 of β-glucose which was also confirmed by a corresponding HMBC correlation.

HPLC-DAD/MS and NMR spectroscopic investigations revealed that the neohesperidin dihydrochalcone preparation contained some residual amounts of two flavonoids which were identified as neohesperidin and diosmin-7-neohesperidoside (peaks marked with an asterisk in Fig. 6B). The monoglucosylated neohesperidin dihydrochalcone conjugate formed by mutant *L. reuteri* TMW 1.106 dextransucrase eluted near the two flavonoids and was therefore only obtained in a mixture with neohesperidin. However, it was possible to assign all HSQC signals corresponding to the aglycone (hesperetin) and the unsubstituted neohesperidose by using COSY and TOCSY experiments. With regards to the monoglucosylated neohesperidin

dihydrochalcone conjugate, the chemical shifts of the HSQC signals derived from the aglycone were comparable to the chemical shifts obtained for unmodified neohesperidin dihydrochalcone. In the anomeric region of the HSQC spectrum, two anomeric signals were detected at 5.10/100.1 ppm and 5.14/97.0 ppm besides the additional signals of a carbohydrate-bound α-glucose unit. The carbon shifts of these two signals were similar to unmodified neohesperidose, therefore the signals can be assigned to β-glucose and α-rhamnose. The assignment of the remaining HSQC signals of these two sugar units showed that the C4H4 signal of the α-rhamnose unit was clearly shifted downfield in the ^{13}C dimension. Furthermore, an HMBC correlation between H1 of α-glucose and C4 of α-rhamnose was found. Therefore, it was possible to conclude that the α-glucose unit is bound to position *O*4 of the α-rhamnose unit.

The structures of the naringin and neohesperidin dihydrochalcone conjugates demonstrate that mutant *L. reuteri* TMW 1.106 dextransucrase is also able to glucosylate flavonoid-bound neohesperidose units. However, naringin was glucosylated at the β-glucose unit and neohesperidin dihydrochalcone was glucosylated at the α-rhamnose unit. These results suggest that the aglycone has a significant influence on the glucosylation position. This may be caused by different orientations of the acceptor substrate in the active site of the dextransucrases. However, just as rutin (R-G1b), neohesperidin dihydrochalcone was glucosylated at position *O*4 of the α-rhamnose unit. Thus, the position to which α-rhamnose is attached seems to be of secondary importance and conjugation of α-rhamnose preferably occurs at position *O*4. However, glucosylation of α-rhamnose was only observed for substrates which lack substitution of the β-glucose unit. Therefore, it is likely that the corresponding conjugates are only formed if the β-glucose units are not in a suitable position in the active site. Furthermore, Na-G1a, which is substituted at position *O*4' of naringin, is a rather uncommon reaction product because

previous studies suggested that glucansucrases prefer vicinal phenolic hydroxyl groups for glucosylation [14, 29].

3.4 Epigallocatechin gallate and dihydromyricetin

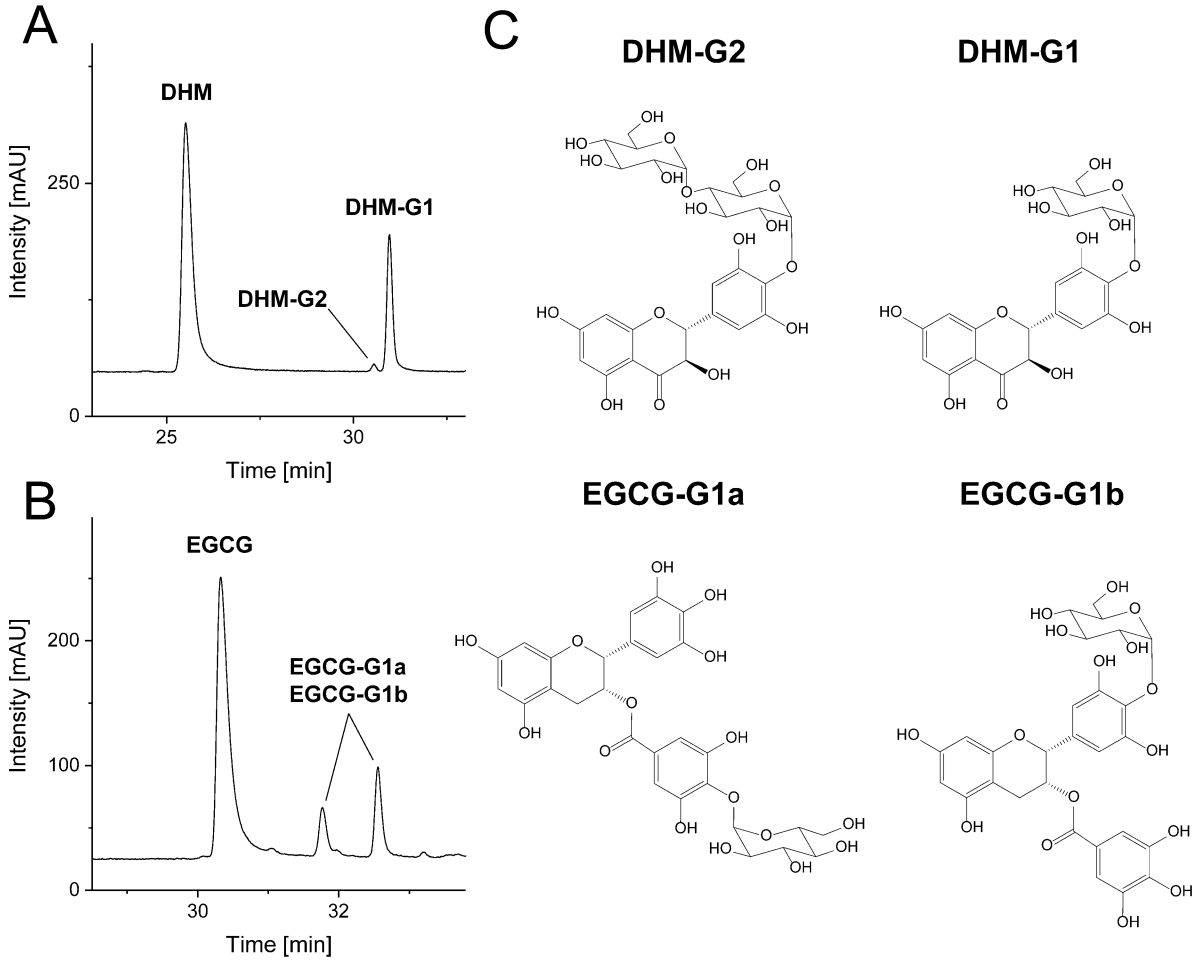

Fig. 7: HPLC-DAD/MS chromatograms of incubations of dihydromyricetin (DHM, final concentration: 30 mM, subfigure A) and epigallocatechin gallate (EGCG, final concentration: 20 mM, subfigure B) with 100 mU / mL mutant *L. reuteri* TMW 1.106 dextransucrase and 500 mM sucrose. The structures of the conjugates (subfigure C) were determined by NMR spectroscopy.

In the incubation mixture of dihydromyricetin, a monoglucosylated conjugate was largely predominant besides low amounts of a diglucosylated conjugate (Fig. 7A). Preparative HPLC allowed for the isolation of both compounds, but both fractions still contained residual unmodified dihydromyricetin. However, signals derived from the additional α-glucose units were clearly assignable because of their different chemical shift.

The HSQC spectrum of the monoglucosylated conjugate DHM-G1 contained the characteristic α-glucose signals as well as one downfield shifted signal in the aromatic region which was identified as the C2'H2' and C6'H6' signals of the conjugated dihydromyricetin. Because glucosylation at position *O*3' / *O*5' would result in two distinct signals, these results suggest that dihydromyricetin is glucosylated at position *O*4'. This was also confirmed by an HMBC correlation between C4' of the conjugated dihydromyricetin and H1 of α-glucose.

For DHM-G2, the chemical shifts of conjugated dihydromyricetin were identical to DHM-G1, thus this conjugate is also substituted at position *O*4'. As expected for a diglucosylated conjugate, two anomeric signals were detected (Fig. S6). The anomeric signal of the dihydromyricetin-bound glucosyl unit was identified based on its chemical shift and an HMBC correlation between H1 and C4' of dihydromyricetin. From the assignment of the remaining HSQC signals, it was demonstrated that the C4H4 signal of the dihydromyricetin-bound α-glucose unit was significantly downfield shifted in the ^{13}C dimension (69.1 to 78.6 ppm). In addition, the chemical shifts of the second glucosyl unit were in good agreement with glycoside-bound, terminal α-glucose. Therefore, DHM-G2 contains a maltosyl unit bound to position *O*4' of the B-ring.

Incubation of epigallocatechin gallate with mutant *L. reuteri* TMW 1.106 dextransucrase yielded two monoglucosylated conjugates which eluted near to each other and also near to unmodified epigallocatechin gallate (Fig. 7B). As a consequence, the two conjugates were only isolated in a mixture with each other and unconjugated epigallocatechin gallate. Thus, the

HSQC spectrum contained two close-by anomeric α-glucose signals (Fig. 8A). However, the five non-anomeric HSQC signals of the two α-glucose units were identical. The aromatic region of the spectrum was dominated by two signals (6.82/108.4 ppm and 6.40/105.2 ppm) which can be assigned to the unconjugated B-ring (C2'H2' / C6'H6') and unconjugated gallic acid (C2''H2'' / C6''H6'') of epigallocatechin gallate. Besides these signals (and the C6H6 / C8H8 signals), one additional signal at 6.48/105.2 ppm was detected. This signal showed a comparable ^{13}C chemical shift than C2'H2'/C6'H6' of the unconjugated B-ring which suggests that one conjugate is substituted at position *O*4'. This was confirmed by an HMBC correlation between the H1 of the glucose unit at 4.83 ppm and the carbon with a chemical shift of 133.3 ppm (red bar in Fig 9B, assigned as C4'). The other α-glucose showed an HMBC correlation between the anomeric proton (5.06 ppm) and a carbon at 137.7 ppm (blue bar in Fig. 8B) which corresponds to C4'' of the ester-bound gallic acid. Therefore, an α-glucose unit is bound to the gallic acid residue, but glucosylation does not impact the proton shift of the substituted gallic acid. This phenomenon was also previously observed by Moon, Kim, Lee, Jin, Kim and Kim [16].

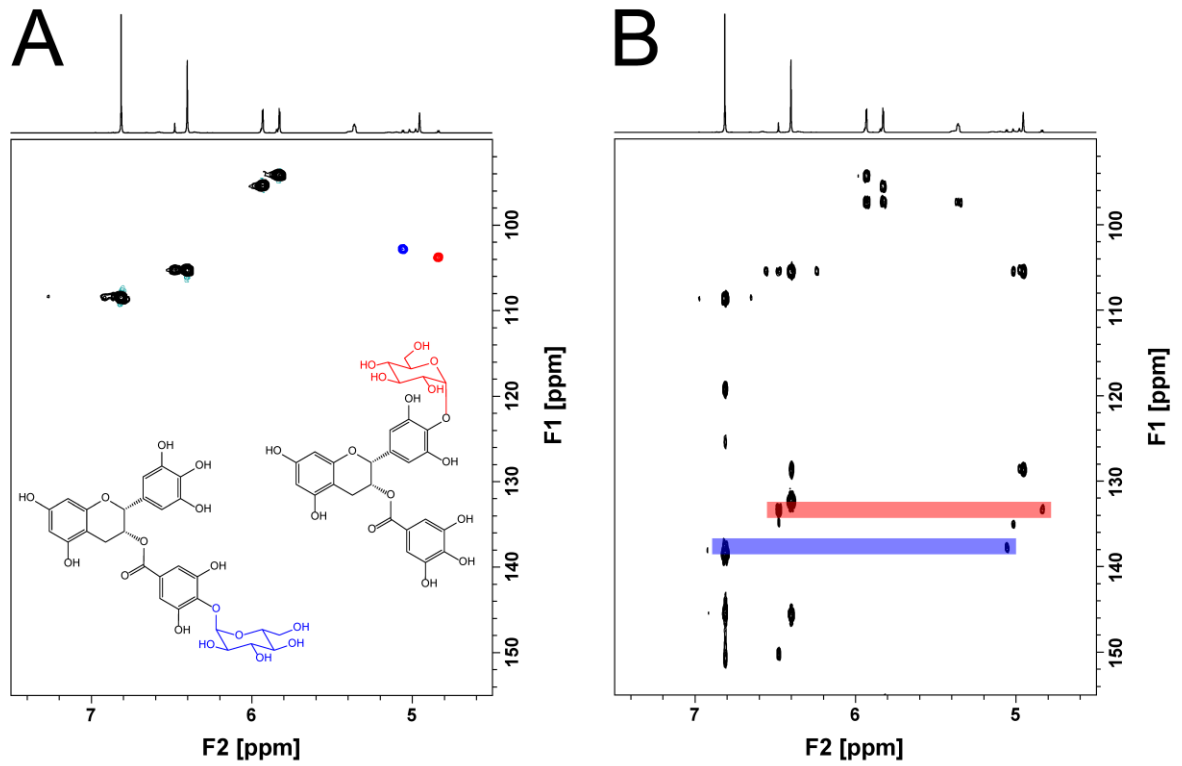

Fig. 8. A: HSQC spectrum and structures of the two monoglucosylated conjugates of epigallocatechin gallate (EGCG-G1a and EGCG-G1b) which were only obtained in a mixture. Signals belonging to the two different α-glucose residues are colored in red and blue. B: HMBC spectrum of the conjugate mixture. Diagnostic correlations between H1 of the α-glucose units and C4' of the B-ring and C4'' of gallic acid are marked by red and blue bars, respectively.

The incubation of dihydromyricetin and epigallocatechin gallate with mutant *L. reuteri* TMW 1.106 dextransucrase demonstrates that flavonoids with a pyrogallol function (located at the B-ring or ester-bound gallic acid) are also efficiently glucosylated by this enzyme. From the structures of the conjugates it can also be derived that pyrogallol functions are preferably glucosylated at position *O*4 as it was also observed for flavonoids with catechol functions. Maltosyl-substituted conjugates were not detected for all substrates but dihydromyricetin, therefore, the formation of this conjugate type is most likely also dependent on the structure of the aglycone. Previous studies on the glucosylation of dihydromyricetin and epigallocatechin

gallate by glucansucrase from *Leuconostoc mesenteroides* B-1299CB also showed preferred glucosylation at position *O*4 of the B-ring and gallic acid [16, 18]. In contrast to the previous studies, oligoglucosylated conjugates or conjugates which are additionally glucosylated at position *O*7 of the flavonoid were not observed in our study. This may be a result of the dextransucrase specificity and or the mutations introduced. However, these results once again demonstrate that mutant *L. reuteri* TMW 1.106 dextransucrase is suitable for effective and specific monoglucosylation without creating high amounts of other products.

3 CONCLUSION

The results of our study demonstrate that mutant *L. reuteri* TMW 1.106 dextransucrase is highly suitable for the synthesis of different flavonoid glucosides. For substrates such as quercetin and its glycosides, a high glucosylation efficiency was achieved, whereas the incubation of e.g. neohesperidin dihydrochalcone and naringin only yielded low portions of glucoconjugates. The different substrates were not only glucosylated with varying efficiencies but also at different positions. While glucosylation of the phenolic hydroxyl groups of the flavonoid B-ring occurred almost exclusively at position *O*4', flavonoid-bound β-glucosyl units were conjugated at position *O*3, *O*4, and *O*6 depending on the substrate. Furthermore, it was possible to demonstrate that flavonoids with a rutinose and a neohesperidose residue can be glucosylated either at position *O*6 of the glucose unit or at position *O*4 of the α-rhamnose unit. Overall, glucosylation by mutant *L. reuteri* TMW 1.106 dextransucrase is highly dependent both on the flavonoid residue and the glycosyl residue. Future studies could evaluate how stability, antioxidant properties, bioavailability, and taste of the conjugates are affected by glucosylation.

4 EXPERIMENTAL

4.1 Materials

Quercetin (≥ 98 %), quercetin-3-*O*-β-glucoside (≥ 98 %), rutin (≥ 97 %), naringin (≥ 98 %), neohesperidin dihydrochalcone (≥ 98 %), epigallocatechin gallate (≥ 98 %), and (if not stated otherwise) all other chemicals were purchased from VWR (Radnor, PA, USA), Sigma Aldrich (Schnelldorf, Germany), Carl Roth (Karlsruhe, Germany), or Carbosynth (Newbury, UK). Cyanidin-3-*O*-β-glucoside was extracted from freeze-dried blackberry powder by using acidic methanol. Anthocyanins were concentrated by solid phase extraction as described previously [30] and purified by preparative HPLC (see below). Dihydromyricetin was obtained from a commercial dietary supplement. pLIC-SGC1 was a gift from Nicola Burgess-Brown (Addgene plasmid # 39187).

4.2 Molecular cloning and site-directed mutagenesis

The gene encoding the previously described dextransucrase from *L. reuteri* TMW 1.106 [27] was amplified from genomic DNA by using a Phusion High-Fidelity PCR kit (Thermo Fisher Scientific, Waltham, MA, USA) and the primers listed in Table S9. The amplified and purified gene was subsequently cloned into the pLIC-SGC1 vector by using a ligation independent cloning approach [31-33]. Site directed mutagenesis of *L. reuteri* dextransucrase was conducted by using a QuikChange Lightning Multi Site-Directed Mutagenesis Kit (Agilent Technologies, Santa Clara, CA, USA) and the mutagenic primer listed in Table S9. After purification, the sequence of the mutagenic plasmid was confirmed by Sanger sequencing (Eurofins GATC Biotech, Konstanz, Germany).

4.3 Heterologous expression

For heterologous expression of the mutated dextransucrase gene, the plasmid was transformed into OneShot BL21 Star (DE3) cells by heat shock. After transferring one colony into 5 mL of

LB medium (100 µg ampicillin / mL), cells were grown at 37 °C and 225 rpm for 6 h. The culture was used to inoculate 200 mL of fresh LB medium (100 µg ampicillin / mL) which was further incubated at 37 °C and 225 rpm for 3 h. After induction of protein expression with isopropyl-β-D-thiogalactopyranoside (final concentration: 0.1 mM), the culture was incubated overnight at room temperature and 225 rpm. Cells were harvested by centrifugation and re-suspended in binding buffer (50 mM sodium phosphate, 300 mM NaCl, 10 mM imidazole, pH 7.5). Lysis of the re-suspended cells was carried out by sonication (amplitude 50 %, 3x 20 s pulse, 59.9 s pause) with a Sonifier W-250 D (Branson, Dabury, CT, USA) and cell debris were removed by centrifugation (30 min, 4 °C, 20000 x g). For purification of the recombinant dextransucrase, the clear supernatant was transferred to a HisPur Ni-NTA resin (Thermo Fisher Scientific; pre-equilibrated with binding buffer) and incubated at 4 °C for 1 h. After washing with 4 volumes of binding buffer, recombinant proteins were eluted with elution buffer (50 mM sodium phosphate, 300 mM NaCl, 100 mM imidazole, pH 7.5) which resulted in a typical yield of 100 mg dextransucrase / L culture. Hydrolytic activity of the recombinant dextransucrase was determined by analyzing the release of *para*-nitrophenol from 35 mM *para*-nitrophenyl-α-glucoside (25 mM sodium acetate buffer, supplemented with 1 mM $CaCl_2$, pH 5.5) in a microplate reader (Infinite M200 PRO, Tecan, Männedorf, Switzerland) at 400 nm. A standard curve was used to calculate the volume activity (1 µmol of released *para*-nitrophenol / min) per µL.

4.4 Acceptor reactions

For glucosylation, quercetin, quercetin-3-*O*-β-glucoside, rutin, cyanidin-3-*O*-β-glucoside, naringin, neohesperidin dihydrochalcone, epigallocatechin gallate, and dihydromyricetin were dissolved in DMSO and four volumes of 25 mM sodium acetate buffer (1 mM $CaCl_2$, pH 5.5) were added. This procedure allowed for solubilization of comparably high amounts of these substrates (quercetin: 3 mM, quercetin-3-*O*-β-glucoside: 5 mM, rutin: 3 mM, cyanidin-3-*O*-β-

glucoside: 8 mM, naringin: 30 mM, neohesperidin dihydrochalcone: 50 mM, epigallocatechin gallate: 20 mM, dihydromyricetin: 30 mM). After the addition of sucrose (final concentration: 500 mM), 100 mU of *L. reuteri* TMW 1.106 L242A dextransucrase / mL substrate solution were added and the mixture was incubated for 24 h at 30 °C. The enzyme was inactivated by heating to 95 °C for 5 min and the mixture was used for further analysis and fractionation.

4.5 Glucoconjugate analysis and purification

For chromatographic analysis of the glucoconjugates, the glucosylation mixtures were diluted and analyzed on a Surveyor HPLC-DAD system coupled to an LXQ linear ion trap MS^n system (Thermo Fisher Scientific). A Kinetex C18 column (100 mm x 4.6 mm i.d., 2.6 µm particle size; Phenomenex, Torrance, CA, USA) and the following gradient composed of water with 0.1 % formic acid (eluent A) and acetonitrile with 0.1 % formic acid (eluent B) were used at 0.5 mL/min and 30 °C: 0-5 min, isocratic 3 % B; 5-25 min, linear to 8 % B; 25-45 min, linear to 28 % B; 45-55 min, linear to 60 % B; 55-56 min, linear to 100 % B; 56-62 min, isocratic 100 % B; 62-64 min, linear to 3 % B; 64-70 min, isocratic 3 % B. For the analysis of cyanidin-3-*O*-β-glucoside, 0.5 % formic acid was added to both eluents. Flavonoids were detected at 280 nm (neohesperidin dihydrochalcone, epigallocatechin gallate, and dihydromyricetin), 320 nm (quercetin, quercetin-3-*O*-β-glucoside, rutin, and naringin), and 510 nm (cyanidin-3-*O*-β-glucoside). For mass spectrometric analysis of the unmodified and conjugated flavonoids, electrospray ionization was used in positive (cyanidin-3-*O*-β-glucoside) and negative (all other compounds) mode. Prior to purification with preparative HPLC, conjugated flavonoids were enriched by using solid phase extraction on a Chromabond C18 (Macherey Nagel, Düren, Germany; preconditioned with methanol and water) stationary phase. The glucosylation mixtures were loaded onto the column, the column was washed with water, and conjugates were eluted by using methanol. Fractionation of the conjugates was conducted on a preparative HPLC-UV system (LC-8A pumps, SPD-20A UV detector, Shimadzu, Kyoto, Japan) equipped

with a Luna C18 column (250 mm × 10 mm i.d., 5 µm particle size, Phenomenex). The same conditions as described above were used at 8 mL/min and room temperature. In some cases, the gradient was truncated to: 0-5 min, linear from 3 % B to 8 % B; 5-25 min linear to 28 % B; 25-35 min, linear to 40 % B; 35-36 min, linear to 100 % B; 36-41 min, isocratic 100 % B; 41-42 min, linear to 3 % B, 42-47 min, isocratic 3 % B. Detection of the conjugates was carried out at 510 nm (cyanidin-3-*O*-β-glucoside) and 280 nm (all other compounds). The resulting fractions were evaporated and freeze-dried.

4.6 NMR spectroscopy

NMR spectroscopic analysis of the standard compounds and conjugates was carried out on an Ascend 500 MHz spectrometer (Bruker, Rheinstetten, Germany) equipped with a Prodigy cryoprobe. Cyanidin-3-*O*-β-glucoside was dissolved in methanol-*d*4 whereas all other conjugates were dissolved in DMSO-*d*6. Chemical shifts were referenced to the solvent residual peak (methanol-*d*4: 3.31 / 49.00 ppm; DMSO-*d*6: 2.50 / 39.52 ppm) according to Gottlieb, Kotlyar and Nudelman [34]. Standard Bruker parameter sets were used to record proton, HSQC, H2BC, COSY, (HSQC-)TOCSY, and HMBC spectra.

ACKNOWLEDGEMENT

The authors are very grateful to Frank Jakob and Rudi Vogel from the Chair of Technical Microbiology (TU Munich) for providing *L. reuteri* TMW 1.106 genomic DNA.

FUNDING

This work was supported by the Carl-Zeiss Foundation.

REFERENCES

[1] P.C.H. Hollman, A. Cassidy, B. Comte, M. Heinonen, M. Richelle, E. Richling, M. Serafini, A. Scalbert, H. Sies, S. Vidry, The biological relevance of direct antioxidant effects of polyphenols for cardiovascular health in humans is not established. J. Nutr. 141 (2011) 989S-1009S. https://doi.org/10.3945/jn.110.131490.

[2] E. Tripoli, M. La Guardia, S. Giammanco, D. Di Majo, M. Giammanco, Citrus flavonoids: Molecular structure, biological activity and nutritional properties: A review. Food Chem. 104 (2007) 466-479. https://doi.org/10.1016/j.foodchem.2006.11.054.

[3] G.E. Inglett, L. Krbechek, B. Dowling, R. Wagner, Dihydrochalcone sweeteners - Sensory and stability evaluation. J. Food Sci. 34 (1969) 101-103. https://doi.org/10.1111/j.1365-2621.1969.tb14371.x.

[4] M. Plaza, T. Pozzo, J.Y. Liu, K.Z.G. Ara, C. Turner, E.N. Karlsson, Substituent effects on *in vitro* antioxidizing properties, stability, and solubility in flavonoids. J. Agric. Food Chem. 62 (2014) 3321-3333. https://doi.org/10.1021/jf405570u.

[5] K. Murota, N. Matsuda, Y. Kashino, Y. Fujikura, T. Nakamura, Y. Kato, R. Shimizu, S. Okuyama, H. Tanaka, T. Koda, K. Sekido, J. Terao, α-Oligoglucosylation of a sugar moiety enhances the bioavailability of quercetin glucosides in humans. Arch. Biochem. Biophys. 501 (2010) 91-97. https://doi.org/10.1016/j.abb.2010.06.036.

[6] X. Zhang, J. Wang, J.M. Hu, Y.W. Huang, X.Y. Wu, C.T. Zi, X.J. Wang, J. Sheng, 2016. Synthesis and biological testing of novel glucosylated epigallocatechin gallate (EGCG) derivatives. Molecules. 21, 620. https://doi.org/10.3390/molecules21050620.

[7] Y.S. Lee, J.B. Woo, S.I. Ryu, S.K. Moon, N.S. Han, S.B. Lee, Glucosylation of flavonol and flavanones by *Bacillus* cyclodextrin glucosyltransferase to enhance their solubility and stability. Food Chem. 229 (2017) 75-83. https://doi.org/10.1016/j.foodchem.2017.02.057.

[8] C. Aoki, Y. Takeuchi, K. Higashi, Y. Okamoto, A. Nakanishi, M. Tandia, J. Uzawa, K. Ueda, K. Moribe, Structural elucidation of a novel transglycosylated compound α-glucosyl rhoifolin and of α-glucosyl rutin by NMR spectroscopy. Carbohydr. Res. 443 (2017) 37-41. https://doi.org/10.1016/j.carres.2017.03.011.

[9] J.S. Cho, S.S. Yoo, T.K. Cheong, M.J. Kim, Y. Kim, K.H. Park, Transglycosylation of neohesperidin dihydrochalcone by *Bacillus stearothermophilus* maltogenic amylase. J. Agric. Food Chem. 48 (2000) 152-154. https://doi.org/10.1021/jf991044y.

[10] J.L. Gonzalez-Alfonso, L. Leemans, A. Poveda, J. Jimenez-Barbero, A.O. Ballesteros, F.J. Plou, Efficient α-glucosylation of epigallocatechin gallate catalyzed by cyclodextrin glucanotransferase from *Thermoanaerobacter* species. J. Agric. Food Chem. 66 (2018) 7402-7408. https://doi.org/10.1021/acs.jafc.8b02143.

[11] T. Kometani, T. Nishimura, T. Nakae, H. Takii, S. Okada, Synthesis of neohesperidin glycosides and naringin glycosides by cyclodextrin glucanotransferase from an alkalophilic *Bacillus* species. Biosci. Biotechnol. Biochem. 60 (1996) 645-649. https://doi.org/10.1271/bbb.60.645.

[12] S.J. Lee, J.C. Kim, M.J. Kim, M. Kitaoka, C.S. Park, S.Y. Lee, M.J. Ra, T.W. Moon, J.F. Robyt, K.H. Park, Transglycosylation of naringin by *Bacillus stearothermophilus* maltogenic amylase to give glycosylated naringin. J. Agric. Food Chem. 47 (1999) 3669-3674. https://doi.org/10.1021/jf990034u.

[13] Y. Suzuki, K. Suzuki, Enzymatic formation of 4G-α-D-glucopyranosyl-rutin. Agric. Biol. Chem. 55 (1991) 181-187. https://doi.org/10.1080/00021369.1991.10870539.

[14] A. Bertrand, S. Morel, F. Lefoulon, Y. Rolland, P. Monsan, M. Remaud-Simeon, *Leuconostoc mesenteroides* glucansucrase synthesis of flavonoid glucosides by acceptor reactions in aqueous-organic solvents. Carbohydr. Res. 341 (2006) 855-863. https://doi.org/10.1016/j.carres.2006.02.008.

[15] G.E. Kim, H.K. Kang, E.S. Seo, S.H. Jung, J.S. Park, D.H. Kim, D.W. Kim, S.A. Ahn, C. Sunwoo, D. Kim, Glucosylation of the flavonoid, astragalin by *Leuconostoc mesenteroides* B-512FMCM dextransucrase acceptor reactions and characterization of the products. Enzyme Microb. Technol. 50 (2012) 50-56. https://doi.org/10.1016/j.enzmictec.2011.09.007.

[16] Y.H. Moon, G. Kim, J.H. Lee, X.J. Jin, D.W. Kim, D. Kim, Enzymatic synthesis and characterization of novel epigallocatechin gallate glucosides. J. Mol. Catal. B: Enzym. 40 (2006) 1-7. https://doi.org/10.1016/j.molcatb.2006.01.030.

[17] Y.H. Moon, J.H. Lee, D.Y. Jhon, W.J. Jun, S.S. Kang, J. Sim, H. Choi, J.H. Moon, D. Kim, Synthesis and characterization of novel quercetin-α-D-glucopyranosides using glucansucrase from *Leuconostoc mesenteroides*. Enzyme Microb. Technol. 40 (2007) 1124-1129. https://doi.org/10.1016/j.enzmictec.2006.08.019.

[18] H.J. Woo, H.K. Kang, T.H.N. Thi, G.E. Kim, Y.M. Kim, J.S. Park, D. Kim, J. Cha, Y.H. Moon, S.H. Nam, Y.M. Xia, A. Kimura, D. Kim, Synthesis and characterization of ampelopsin glucosides using dextransucrase from *Leuconostoc mesenteroides* B-1299CB4: Glucosylation enhancing physicochemical properties. Enzyme Microb. Technol. 51 (2012) 311-318. https://doi.org/10.1016/j.enzmictec.2012.07.014.

[19] Y. Malbert, S. Pizzut-Serin, S. Massou, E. Cambon, S. Laguerre, P. Monsan, F. Lefoulon, S. Morel, I. Andre, M. Remaud-Simeon, Extending the structural diversity of α-flavonoid glycosides with engineered glucansucrases. ChemCatChem 6 (2014) 2282-2291. https://doi.org/10.1002/cctc.201402144.

[20] Y. Malbert, C. Moulis, Y. Brison, S. Morel, I. Andre, M. Remaud-Simeon, 2018. Engineering a branching sucrase for flavonoid glucoside diversification. Sci. Rep. 8, 15153. https://doi.org/10.1038/s41598-018-33394-y.

[21] H. Leemhuis, T. Pijning, J.M. Dobruchowska, S.S. van Leeuwen, S. Kralj, B.W. Dijkstra, L. Dijkhuizen, Glucansucrases: Three-dimensional structures, reactions, mechanism, α-glucan analysis and their implications in biotechnology and food applications. J. Biotechnol. 163 (2013) 250-272. https://doi.org/10.1016/j.jbiotec.2012.06.037.

[22] G.J. Gerwig, E.M. te Poele, L. Dijkhuizen, J.P. Kamerling, Structural analysis of rebaudioside A derivatives obtained by *Lactobacillus reuteri* 180 glucansucrase-catalyzed trans-α-glucosylation. Carbohydr. Res. 440-441 (2017) 51-62. https://doi.org/10.1016/j.carres.2017.01.008.

[23] E.M. te Poele, T. Devlamynck, M. Jager, G.J. Gerwig, D. Van de Walle, K. Dewettinck, A.K.H. Hirsch, J.P. Kamerling, W. Soetaert, L. Dijkhuizen, 2018. Glucansucrase (mutant) enzymes from *Lactobacillus reuteri* 180 efficiently transglucosylate Stevia component rebaudioside A, resulting in a superior taste. Sci. Rep. 8, 1516. https://doi.org/10.1038/s41598-018-19622-5.

[24] T. Devlamynck, E.M. te Poele, K. Quataert, G.J. Gerwig, D. Van de Walle, K. Dewettinck, J.P. Kamerling, W. Soetaert, L. Dijkhuizen, Trans-α-glucosylation of stevioside by the mutant glucansucrase enzyme Gtf180-Delta N-Q1140E improves its taste profile. Food Chem. 272 (2019) 653-662. https://doi.org/10.1016/j.foodchem.2018.08.025.

[25] E.M. te Poele, P. Grijpstra, S.S. van Leeuwen, L. Dijkhuizen, Glucosylation of catechol with the GTFA Glucansucrase enzyme from *Lactobacillus reuteri* and sucrose as donor substrate. Bioconjugate Chem. 27 (2016) 937-946. https://doi.org/10.1021/acs.bioconjchem.6b00018.

[26] T. Devlamynck, E.M. te Poele, X.F. Meng, S.S. van Leeuwen, L. Dijkhuizen, Glucansucrase Gtf180-Delta N of *Lactobacillus reuteri* 180: Enzyme and reaction engineering for improved glycosylation of non-carbohydrate molecules. Appl. Microbiol. Biotechnol. 100 (2016) 7529-7539. https://doi.org/10.1007/s00253-016-7476-x.

[27] C. Rühmkorf, C. Bork, P. Mischnick, H. Rübsam, T. Becker, R.F. Vogel, Identification of *Lactobacillus curvatus* TMW 1.624 dextransucrase and comparative characterization with *Lactobacillus reuteri* TMW 1.106 and *Lactobacillus animalis* TMW 1.971 dextransucrases. Food Microbiol. 34 (2013) 52-61. https://doi.org/10.1016/j.fm.2012.11.002.

[28] F. Münkel, D. Wefers, Fine structures of different dextrans assessed by isolation and characterization of endo-dextranase liberated isomalto-oligosaccharides. Carbohydr. Polym. 215 (2019) 296-306. https://doi.org/10.1016/j.carbpol.2019.03.027.

[29] G.H. Meulenbeld, S. Hartmans, Transglycosylation by *Streptococcus mutans* GS-5 glucosyltransferase-D: Acceptor specificity and engineering of reaction conditions. Biotechnol. Bioeng. 70 (2000) 363-369. https://doi.org/10.1002/1097-0290(20001120)70:4<363::aid-bit1>3.0.co;2-2.

[30] G. Skrede, R.E. Wrolstad, R.W. Durst, Changes in anthocyanins and polyphenolics during juice processing of highbush blueberries (*Vaccinium corymbosum* L.). J. Food Sci. 65 (2000) 357-364. https://doi.org/10.1111/j.1365-2621.2000.tb16007.x.

[31] C. Aslanidis, P.J. Dejong, Ligation-independent cloning of PCR products (LIC-PCR). Nucleic Acids Res. 18 (1990) 6069-6074. https://doi.org/10.1093/nar/18.20.6069.

[32] L. Stols, M.Y. Gu, L. Dieckman, R. Raffen, F.R. Collart, M.I. Donnelly, A new vector for high-throughput, ligation-independent cloning encoding a tobacco etch virus protease cleavage site. Protein Expression Purif. 25 (2002) 8-15. https://doi.org/10.1006/prep.2001.1603.

[33] N.A. Burgess-Brown, S. Sharma, F. Sobott, C. Loenarz, U. Oppermann, O. Gileadi, Codon optimization can improve expression of human genes in *Escherichia coli*: A multi-gene study. Protein Expression Purif. 59 (2008) 94-102. https://doi.org/10.1016/j.pep.2008.01.008.

[34] H.E. Gottlieb, V. Kotlyar, A. Nudelman, NMR chemical shifts of common laboratory solvents as trace impurities. J. Org. Chem. 62 (1997) 7512-7515. https://doi.org/10.1021/jo971176v.

HIGHLIGHTS

- Multiple flavonoids were glucosylated by using a mutant *L. reuteri* dextransucrase
- The B-ring of different flavonoids was preferably glucosylated at position *O*4
- Flavonoid-bound glucose units were glucosylated at varying positions
- Rutinose and neohesperidose units were glucosylated at position *O*4 of rhamnose
- Glucosylation positions and extent greatly depend on the structure of the substrate